Bulletin of the Geological Survey of Japan, vol.60 (1/2), p.117-130, 2009

Article

Geological model of the Yellow River basin for the long-term groundwater simulation

Hirofumi Muraoka[1], Koji Mori[2], Shiro Tamanyu[3], Takemasa Ishii[1] and Youhei Uchida[1]

Hirofumi Muraoka, Koji Mori, Shiro Tamanyu, Takemasa Ishii and Youhei Uchida (2009) Geological model of the Yellow River basin for the long-term groundwater simulation. *Bull. Geol. Surv. Japan*, vol. 60 (1/2), p. 117-130, 12 figs.

Abstract: To simulate long-term groundwater flow within the whole catchment areas of the Yellow River basin, a hydrogeological model is formulated. This model includes the impermeable basement defined by the brittle-plastic transition, formulation of the depth-dependency of permeability of the upper crust, major fault distribution, and an isopach map of the Quaternary System. The Yellow River basin is characterized by five stepwise altitude areas; the Tibet Plateau, the northeastern slope of the Tibet Plateau, the northwestern Ordos Plateau, the southeastern slope of the Ordos Plateau and the North China Basin. The structure was formed by tectonics, particularly by the rigid Ordos Micro-Plate block. When adequate permeability and local groundwater consumptions are assumed, the results of the simulation are well consistent with the records of the dramatic decline of the water table since 1960s, indicating the excess groundwater consumptions as the major factor for the decline. This simulator enables to forecast the future shortage of groundwater in the Yellow River basin.

Keywords: Yellow River, groundwater, hydrogeological model, permeability, depth-dependency, impermeable basement

1. Introduction

The central motif of the Yellow River Groundwater Project is to simulate the long-term groundwater flow along the whole catchment of the Yellow River basin in the past as well as in the future. For this purpose, boundary conditions for the three-dimensional permeability structure in the upper crust are critically important. However, the whole catchment areas of the Yellow River basin cover a vast area, about 2300 km east to west and 1000 km north to south, where geology consists of from the Archean to Quaternary Systems and is very complicated. This requires a detailed geological model on one hand, but inevitably requires adequate simplification of the complicated geological structure on the other hand.

This paper describes a model of the boundary conditions for the three-dimensional permeability structure for the simulation of the long-term groundwater flow within the whole catchment areas of the Yellow River basin, including the method to simplify the complicated geology in the given area.

2. General Model for Permeability

2.1 Definition of the impermeable basement

The objective area is here defined from the latitude 33º to 42 º and the longitude 99 º to 121 º as shown in Fig. 1. When we consider such a vast extent of a basin into simulation, we should take an adequate extent to the vertical dimension into account for permeability structure, otherwise the simulation will lose three-dimensional meaning for fluid circulation in a too thin veneer. We thus decided to give an adequate extent is defined by the impermeable basement.

All the rocks will lose the permeability at depth of the brittle-plastic transition below which all the fractures and pores will be closed by viscous behavior of rocks (Fournier, 1991; Muraoka *et al*., 1998, 1999; Muraoka and Ohtani, 2000). The impermeable basement, thus,

[1] AIST, Geological Survey of Japan, Institute for Geo-Resources and Environment, Central 7, Higashi 1-1-1, Tsukuba, Ibaraki, 305-8567 Japan

[2] Geosphere Environmental Technology Corp., Nihonbashi 1-20-8, Chuo-ku, Tokyo, 103-0027 Japan

[3] AIST, Geological Survey of Japan, Geological Museum, Central 7, Higashi 1-1-1, Tsukuba, Ibaraki, 305-8567 Japan

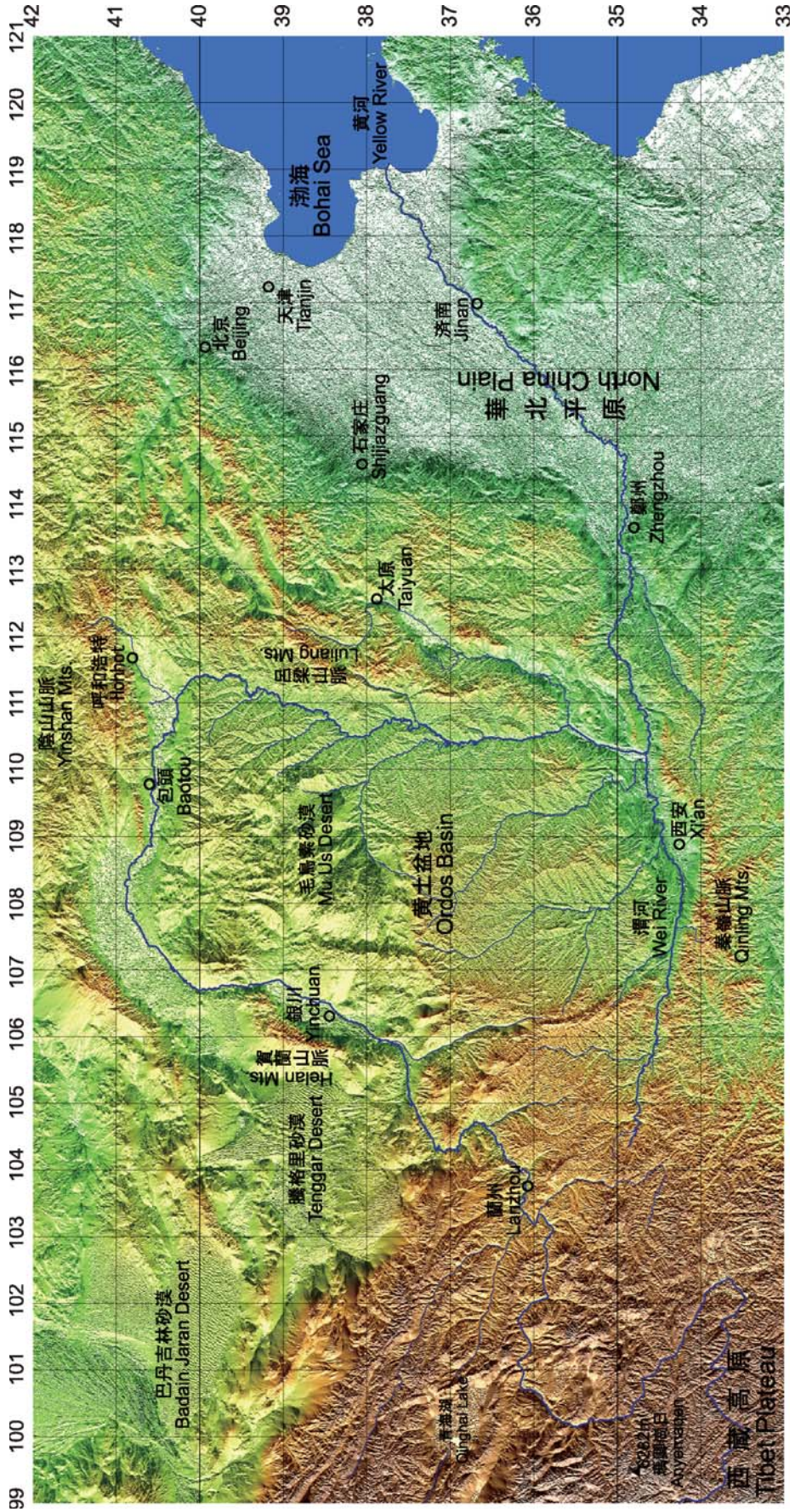

Fig. 1 Topographic base map for the Yellow River basin. Data drawn by the software Kashmir 3D and the digital elevation data SRTM 30.

is the hydrological basement. Because fractures can only occur in the brittle crust, this also means the non-fracture basement.

For simplicity, the top of the impermeable basement, the brittle-plastic transition, is here defined by the temperature of rocks at 380 ºC (Muraoka *et al*., 1998). Strictly speaking, the brittle-plastic transition also depends on the strain rate and rock species, but these factors are not easily available at a greater depth and so it is empirically assumed that the brittle-plastic transition is most effectively controlled by the temperature.

To define the depth of the top of the impermeable basement, a geothermal gradient map is necessary. Hu *et al*. (2000) published a heat flow map of the continental China as shown in Fig. 2. A geothermal gradient can roughly be estimated from a mean thermal conductivity of rocks at 0.004 cal cm^{-1} sec^{-1} ºC. For example, geothermal gradients 60 mWm^{-2}, 80 mWm^{-2}, 100 mWm^{-2} and 150 mWm^{-2} are estimated to be 36 ºC/km, 48 ºC/km, 60 ºC/km and 90 ºC/km, respectively. If mean atmospheric temperature at the ground surface is assumed to be 10 ºC, we can estimate the depth of the top of the impermeable basement D_p in kilometer from the contours in Fig. 2 and the following equation;

$$D_p=(T_p-T_s)/(H_f\,60/100) \quad (1)$$

where T_p is the temperature of the brittle-plastic transition 380 ºC, T_s is the mean atmospheric temperature at the ground surface 10 ºC, and H_f is the heat flow value in the unit mWm^{-2}. Based on the equation, the depth of the top of the impermeable basement is estimated to be 4.1 km for 150 mWm^{-2}, 6.2 km for 100 mWm^{-2}, 7.7 km for 80 mWm^{-2}, and 10.3 km for 60mWm^{-2}. Because the most common heat flow value along the Yellow River basin is between 80 mWm^{-2} and 60mWm^{-2} (Fig. 2), the most common depth of the top of the impermeable basement is estimated to be 10.3 km to 7.7 km.

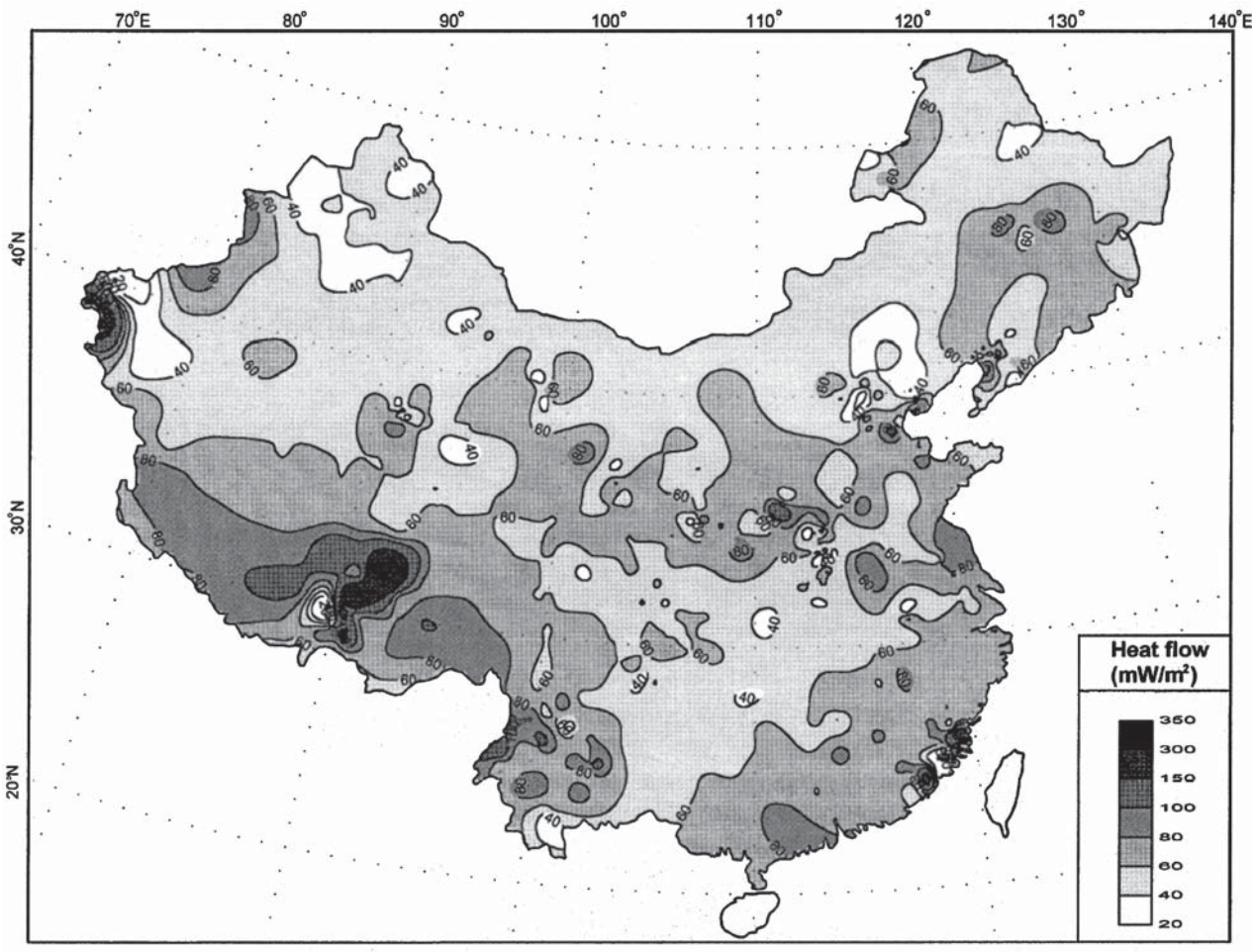

Fig. 2 Heat flow map of continental China after Hu *et al*. (2000). Contour lines are labeled in mWm^{-2}.

2.2 Model for the depth-dependency of permeability

Little has been published on the geological structure along the Yellow River basin at a greater depth. We need, more or less, a general approach on the permeability model at a greater depth. Manning and Ingebritsen (1999) proposed a depth-dependency model of permeability for the continental crust as shown in Fig. 3. It is obvious that there is a depth- (or pressure-) dependency of permeability of rocks at a wider depth range (Fig. 3). As already mentioned, the most common depth of the top of the impermeable basement along the Yellow River basin is estimated to be 10.3 km to 7.7 km. Permeability of rocks is most variable at a depth less than 10 km as seen in Fig. 3. The permeability at a depth less than 10 km is thus a main concern in this study.

Manning and Ingebritsen (1999) described that the permeability-depth curve in Fig. 3 represents the maximum attained at mid to lower crustal levels. In the equation of their regression curve, the permeability is given by the unit m^2 and the depth is given by the unit km. If we convert the depth Z to the SI unit meter and the permeability k to millidarcy md, the equation is given as follows;

$$k = 10\text{^}(10.6 - 3.2\log_{10} Z) \quad (2)$$

The permeability-depth curve in Fig. 3 converges on 10^{-4} md (10^{-19} m^2) at a depth of 35 km. In addition, the smallest value of the error bars is close to 10^{-5} md (10^{-20} m^2). The permeability value 10^{-5} md (10^{-20} m^2), thus, be virtually ascribed into the smallest value in the crust. If we accept this assumption, a general pattern of depth-dependency of permeability of rocks is represented by the logarithmically proportional partitioning between the value 10^{-5} md (10^{-20} m^2) and equation (2) by the following equation;

$$k = 10\text{^}(\log_{10}(10\text{^}(-5)) + a(\log_{10}(10\text{^}(10.6 - 3.2\log_{10} Z)) - \log_{10}(10\text{^}(-5)))) \quad (3)$$

where a is the value from 0 to 1 that is the coefficient of logarithmically proportional partitioning. When we substitute a for the value from 0.2 to 1.0, a model of the depth-dependency of permeability of rocks can be shown in Fig. 4. When we obtain a permeability value at a shallow depth, we can draw a general pattern of the permeability-depth curves and can estimate the permeability value at a greater depth, using this method.

3. Geological Model for Permeability

Owing to the method for the simplification described above, most of deeper geological units can come to be generally treated. Then, we only classified hydrogeologically essential geological units: major faults, Quaternary System and pre-Quaternary System. A topographic base map was composed by the free software Kashmir 3D and the free digital topographic elevation data SRTM 30 released from the United States Geological Survey (USGS) as shown in Fig. 1. All the essential data have been compiled on the three large-scale maps: western, central and eastern maps bounded by latitude 33º to 42 º, longitude 99 º to 107 º: latitude 33º to 42 º, longitude 106 º to 114 º: and latitude 33º to 42 º, longitude 113 º to 121 º, respectively.

3.1 Major fault model

To compile the major faults, we have referred to many literatures (Molnar and Tapponier, 1975; Darby and Ritts, 2002; Jolivet *et al*., 2001; Liu, 1998; Ritts *et al*., 2001; Shao and Wang, 1989; Tapponnier *et al*., 2001; Zhang *et al*., 1998, 2003). The resolutions of the SRTM topographic data are high enough to extract the major fault traces and many faults were also directly

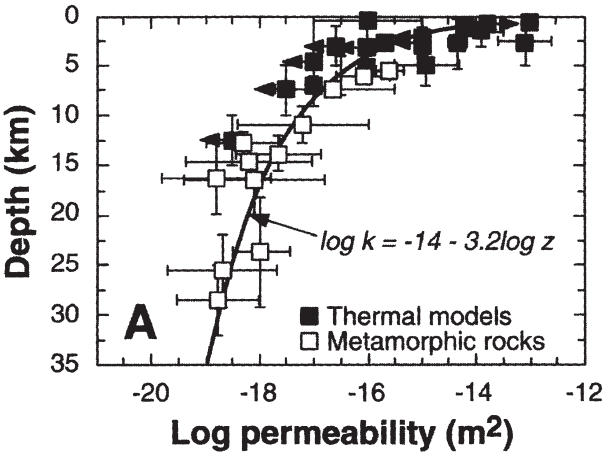

Fig. 3 Permeability as a function of depth in the continental crust after Manning and Ingebritsen (1999).

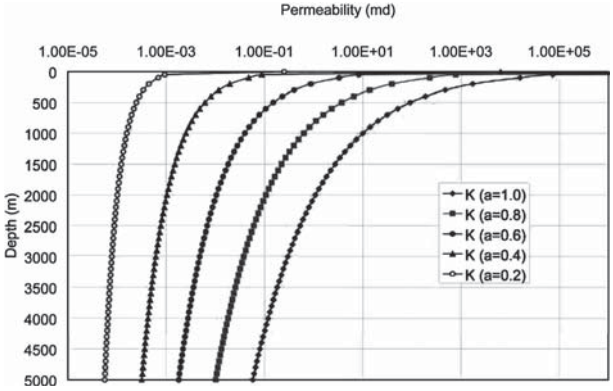

Fig. 4 Generalized pattern of permeability as a function of depth in the continental crust.

depicted from the topographic base maps. We have also classified these faults into the normal faults, strike-slip faults and reverse faults based on the literatures and observation of the topographic base maps. The results are shown in Figs. 5 to 7.

Dip angles of some of these faults are known by detailed studies, but those of many others are not known. For this reason, dip angles of the faults are simplified from known data that those of normal faults are 70 degree, those of strike-slip faults are vertical, and those of reverse faults are 50 degree as shown in Fig. 8.

3.2 Quaternary isopach model

To compile the isopach model for the Quaternary System, we have referred to many literatures (Darby and Ritts, 2002; Liu, 1998; Ritts *et al*., 2001; Shao and Wang, 1989; Zhang *et al*., 1998, 2003). Particularly, the isopach model for the Quaternary System in North China Basin has been referred to a comprehensive published map by Shao and Wang (1989). The compiled results are shown in Figs. 5 to 7.

The maximum thickness of the Quaternary System in North China Basin is about 500 m+ (Shao and Wang, 1989). The data are not available for the Tenggar and Badain Jaran Deserts where the thickness of the Quaternary System was extrapolated from the topography in the surrounding areas and is estimated to be 500 m+ at the maximum. Loess formations are widely distributed in the Ordos Basin where the thickness of loess formations is available but that of the Quaternary System is not available. Therefore, the maximum thickness of the Quaternary System in the Mu Us desert is estimated from the topography to be 400 m+ at the maximum. The Ordos Micro-Plate is surrounded by many grabens reflecting the extension tectonics where the unusually thick Quaternary System was buried (Zhang *et al*., 1998, 2003). For example, the maximum thickness of the Quaternary System is 2,400 m+ in Linhe Trough, 2,000 m+ in Yinchuan Graben, 1,800 m+ in Hohhot Trough and 1,100+ in Weihe Graben (Figs. 5 to 7). Deep groundwater circulations are expected in these areas.

3.3 Allocation of permeability values

Based on the definition and classification described above, permeability units are classified into four major units: the impermeable basement, pre-Quaternary System, Quaternary System and major faults. The impermeable basement is defined by the zero value in the permeability. The depth of the top of the impermeable basement is less than 7.7 km in the shallowest place and larger than 10.3 km in the deepest place in the Yellow River basin. Permeability of the pre-Quaternary System, Quaternary System and major faults increases in this order and all the permeability values are depth-dependent.

We also investigated on the absolute values for each permeability unit, but the actual absolute value is determined by try and error in the process of simulation.

4. Discussion and Conclusions

This study has been done to formulate the boundary conditions for the simulation and is not a self-completed work. The results of the simulation will be described in this issue by Mori *et al*. (2008). According to Mori *et al*. (2008), when adequate permeability and local groundwater consumptions are assumed, the results of the simulation are well consistent with the records of the dramatic decline of the water table since 1960s. This simulator enables to forecast the future shortage of groundwater in the Yellow River basin. If the simulation succeeds, a goal of this study is attained. However, we here discuss general characteristics along the Yellow River basin based on the complied maps (Figs. 5-7).

In terms of the altitude distribution shown in Fig. 9, the Yellow River basin is stepwise classified into three flat areas and two slope areas: the Tibet Plateau as the highest flat, the northeastern slope of the Tibet Plateau as the steepest slope, the northwestern Ordos Plateau as the middle flat, the southeastern slope of the Ordos Plateau as the middle slope and the North China Basin as the lowest flat (Fig. 9).

It should be noted that the altitude distribution is formed by the tectonic activity during the late Cenozoic age (Figs. 5 to 7). As pointed out by Tapponnier *et al*. (2001), the Tibet Plateau is still growing northeastward. This effect caused uplift of the Lanzhou area, resulting in that the Yellow River once changed its course from the present Wei River, a short-cut course, to the present Yellow River, a long detour, at about 8 million years ago (Lin *et al*., 2001). On the other hand, the Ryukyu arc is known to be moving southeastward and forming an extensional subduction zone (Ito *et al*., 1999). As a result, the Yellow River basin is subjected to typical compression tectonics in the upper reach and typical extension tectonics in the lower reach. This regional tectonic situation is well illustrated by the current GPS data as shown in Fig. 10 (Wang and Ye, 2006).

Among the tectonic gradation from the west to east, particularly important is the role of the Ordos Micro-Plate which is an isolated rigid block and is free from the surrounding block. Combining Figs. 7 to 8, a fault map covering the whole area is obtained (Fig. 11). As shown in this map, areas of normal faults and reverse faults are clearly distinguished as an extension tectonic field and a contraction tectonic field, respectively. This reflects the tectonic gradation from the west to east (Fig. 10). Here, the eastern border of the Ordos Micro-Plate should be defined by a series of grabens rather than by the Yellow River as shown by the thick purple line in

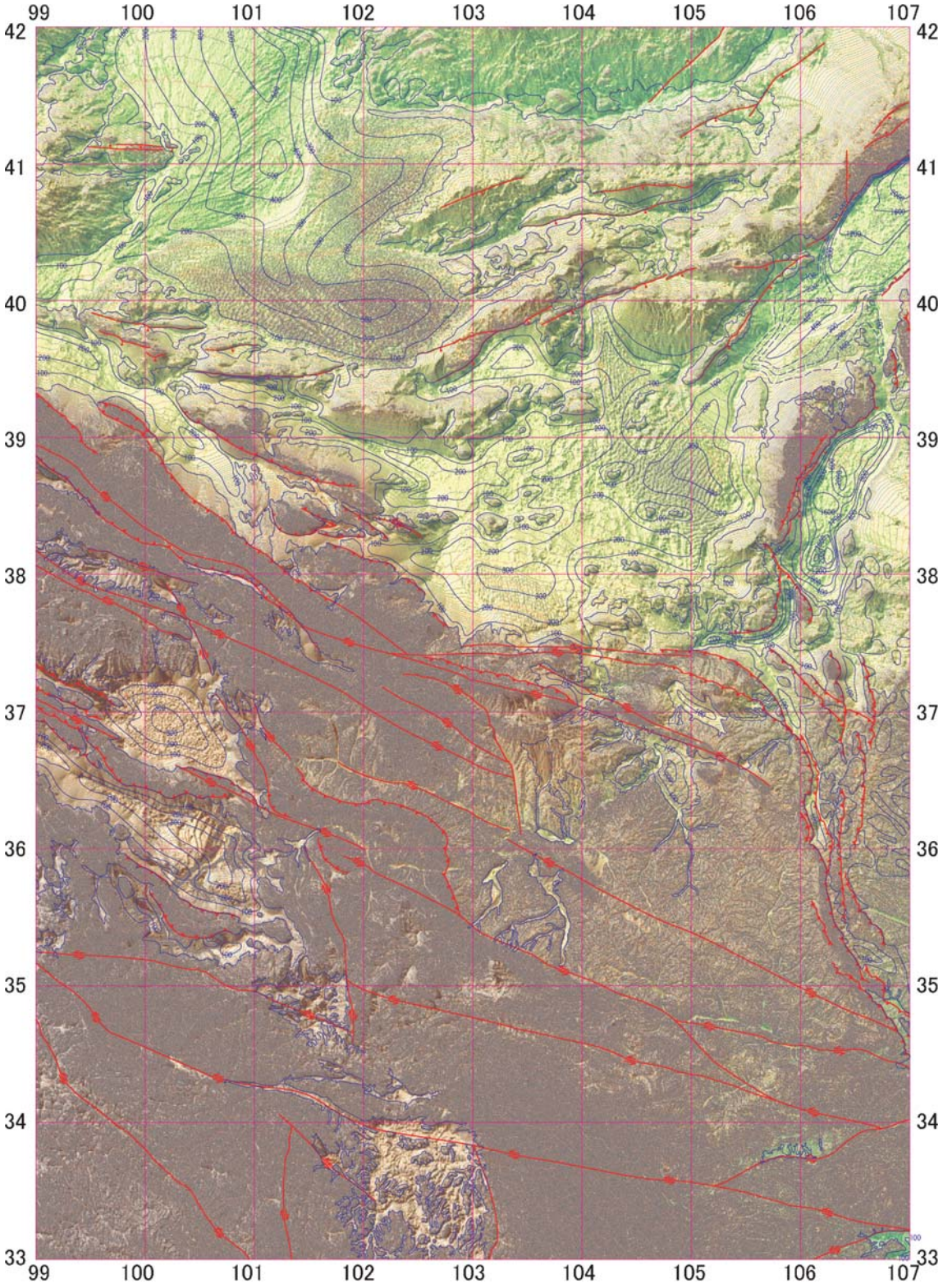

Fig. 5 Compiled major faults and the Quaternary isopach map in the western part of the Yellow River basin.

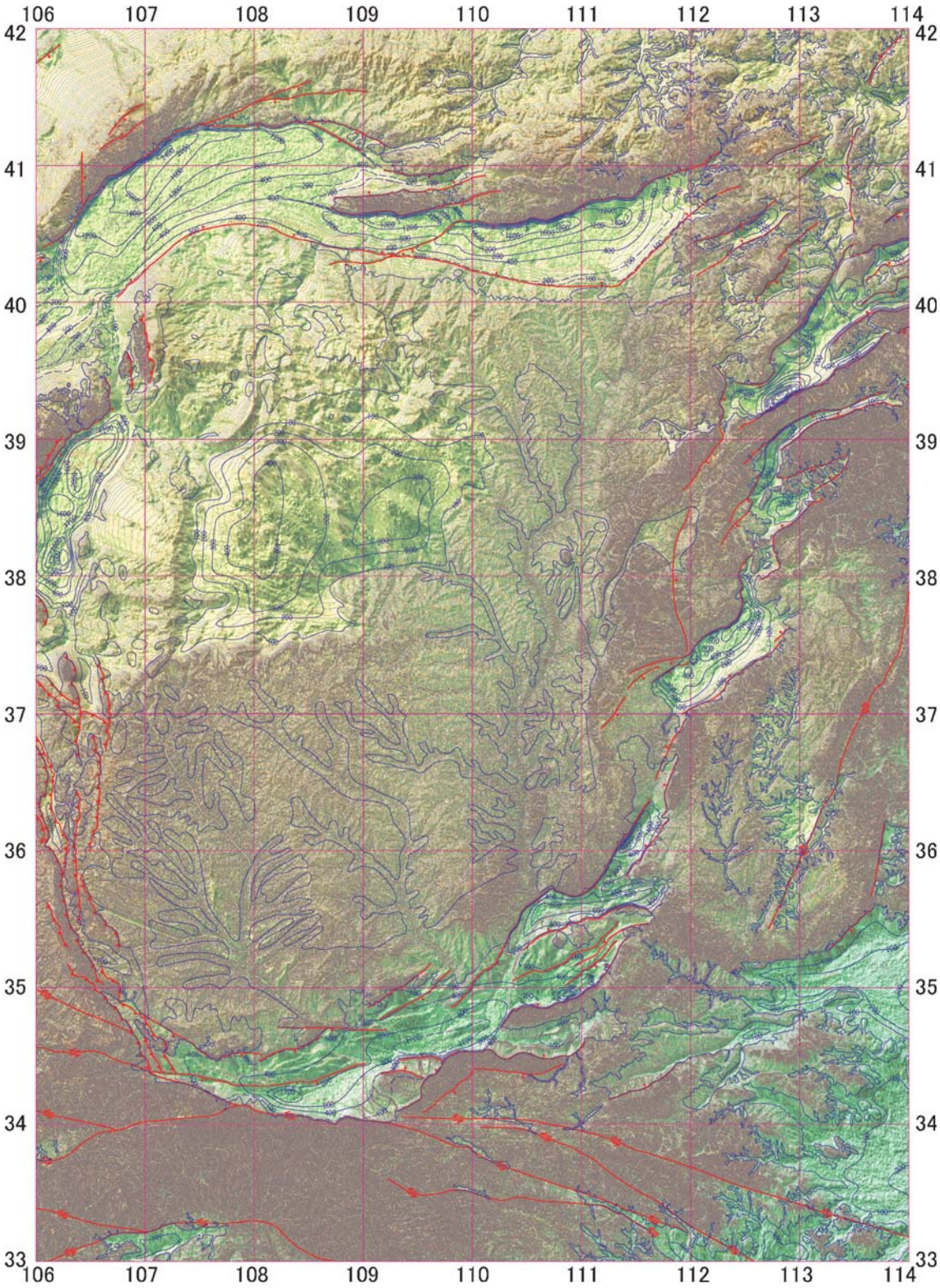

Fig. 6 Compiled major faults and the Quaternary isopach map in the central part of the Yellow River basin.

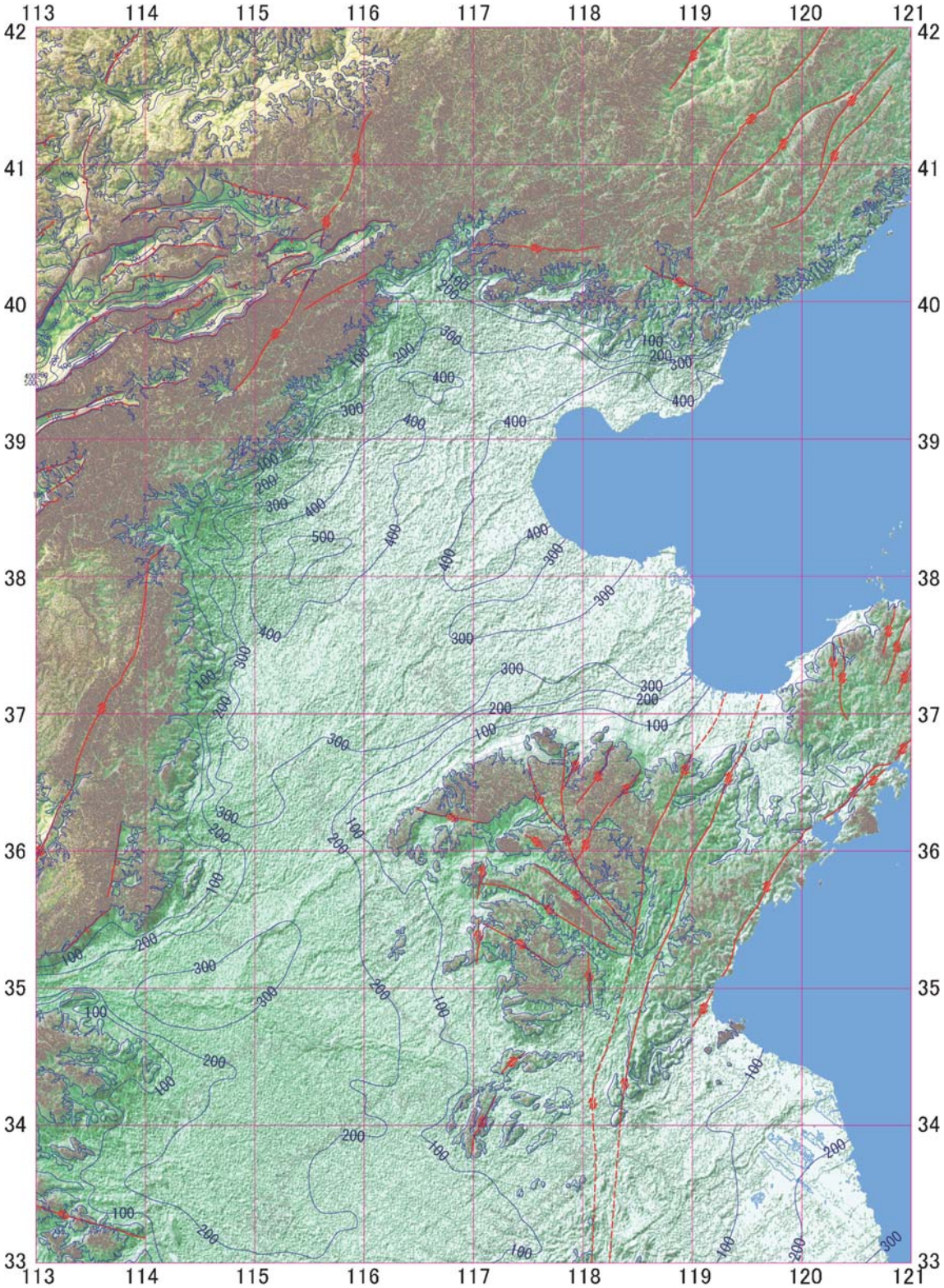

Fig. 7 Compiled major faults and the Quaternary isopach map in the eastern part of the Yellow River basin.

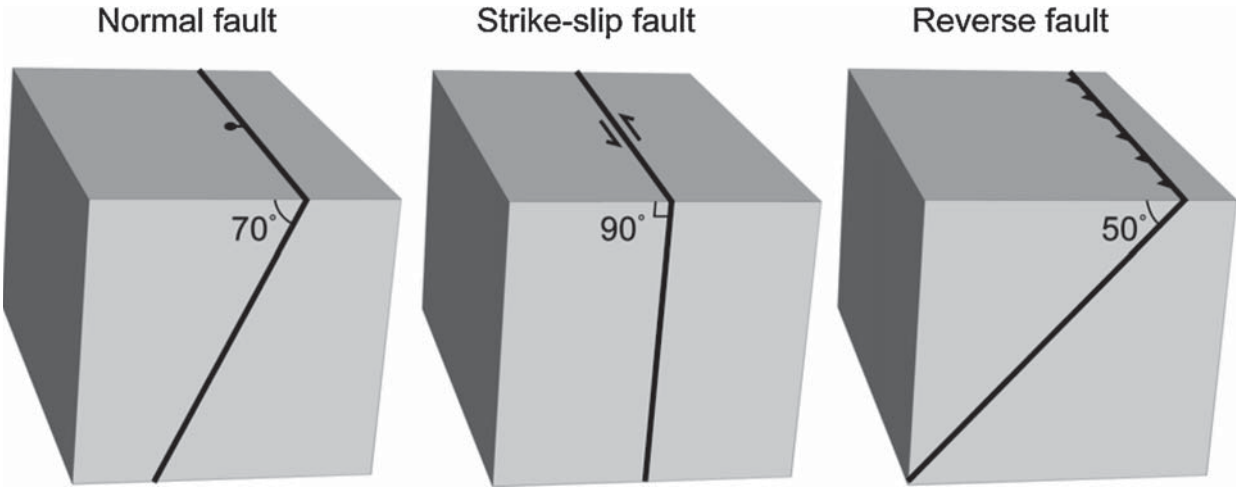

Fig. 8 Simplified dip angles of major faults.

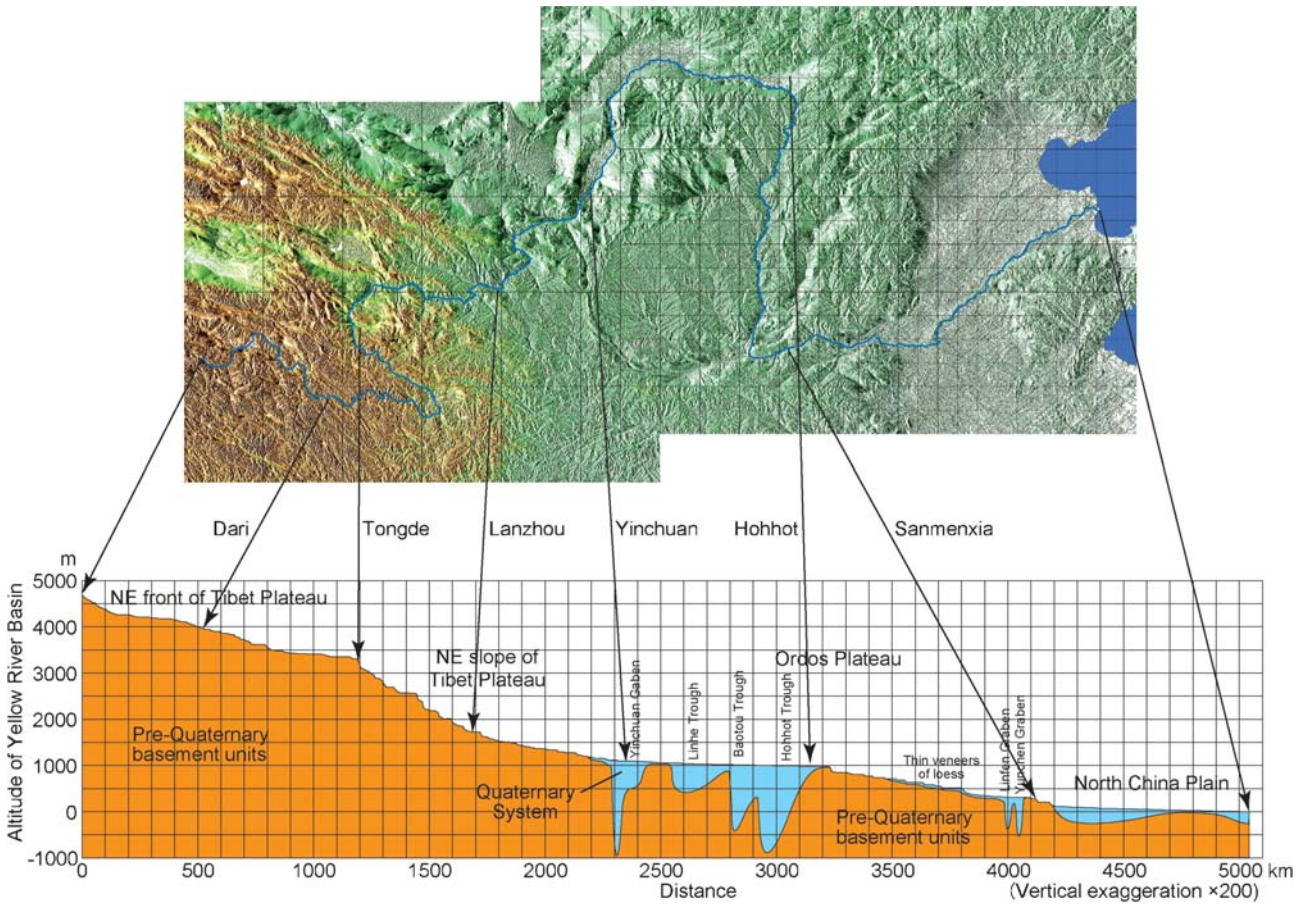

Fig. 9 Altitude and the Quaternary distribution along the Yellow River basin.

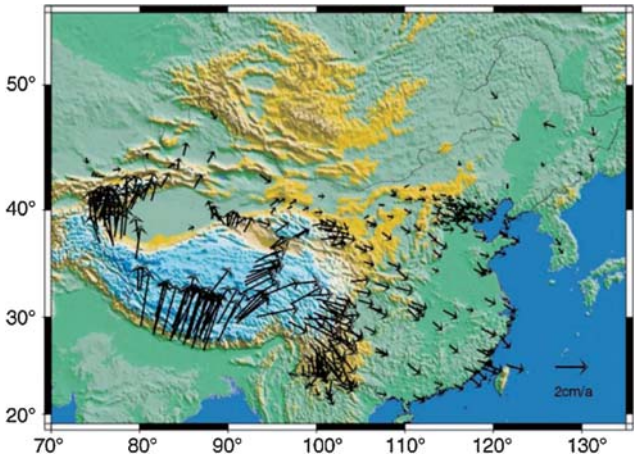

Fig. 10 The averaged GPS velocity field in China (1991-1999) with respect to stable Eurasia after Wang and Ye (2006). Arrows denote the observed GPS velocity vectors.

Fig. 11. This is actually demonstrated by the seismicity in Fig. 12 (Gao *et al*., 1995). Because of the role of the isolated rigid block, compression tectonics completely cease at the western boundary of the Ordos Micro-Plate and extension tectonics initiate from the boundary to the east. Thus many extensional deep grabens are developed in the surroundings of the Ordos Micro-Plate, particularly at the foot of the northeastern slope of the Tibet Plateau. The foot of the northeastern slope of the Tibet Plateau not only has the extensive provenance for the sediments supply on the upper reach but also has the deep tectonic basins for their deposition. This tectonic setting provides the unusually thick Quaternary System as extensive groundwater reservoir in the northwestern Ordos Plateau (Fig. 9). A similar role of the rigid Ordos Micro-Plate is again observed at the southeastern boundary of the Plate (Fig. 9).

The Quaternary System in the North China Basin is not as thick as that of the Ordos Basin, but is characterized by its width and high precipitation. Therefore, in terms of hydrogeological point of view, the Yellow River basin is blessed with extensive natural groundwater storage systems. Recent serious shortage of surface and groundwater is solely ascribed to excessive consumption as compared to their renewable amounts.

References

Darby, B.J. and Ritts, B.D. (2002) Mesozoic contractional deformation in the middle of the Asian tectonic collage: the intraplate Western Ordos fold-thrust belt, China. *Earth and Planetary Science Letters*, **205**, 13-24.

Fournier, R.O. (1991): The transition from hydrostatic to greater than hydrostatic fluid pressure in presently active continental hydrothermal systems in crystalline rock. *Geophysical Research Letters*, **18**, 6248-6252.

Gao, W., Chen, Z. and Xie, X., (1995): The fundamental characteristics of active faults in China. *Quaternary International*, **25**, 13-17.

Hu, S., He, L. and Wang, J. (2000): Heat flow in the continental area of China: a new data set. *Earth and Planetary Science Letters*, **179**, 407-419.

Ito, T., Yoshioka, S. and Miyazaki, S. (1999) Interplate coupling in southwest Japan deduced from inversion analysis of GPS data. *Physics of the Earth and Planetary Interiors*, **115**, 17-34.

Jolivet, M., Brunel, M., Seward, D., Xu, Z., Yang, J., Roger, F., Tapponnier, P., Malavieille, J., Arnaud, N. and Wu, C. (2001) Mesozoic and Cenozoic tectonics of the northern edge of the Tibetan plateau: fission-track constraints. *Tectonophysics*, **343**, 111-134.

Lin, A., Yang, Z., Sun, Z. and Yang, T. (2001): How and when did the Yellow River develop its square bend? *Geology*, **29**, 951-954.

Liu, S. (1998) The coupling mechanism of basin and orogen in the western Ordos Basin and adjacent regions of China. *Journal of Asian Earth Sciences*, **16**, 369-383.

Manning, C.E. and Ingebritsen, S.E. (1999): Permeability of the continental crust: Implications of geothermal data and metamorphic systems. *Reviews of Geophysics*, **37**, 127-150.

Molnar, P. and Tapponnier, P. (1975): Cenozoic tectonics of Asia: Effects of a continental collision. *Science*, **189**, 419-426.

Mori, K., Tada, K. and Nishioka, T. (2008) Large-scale and high-performance groundwater flow

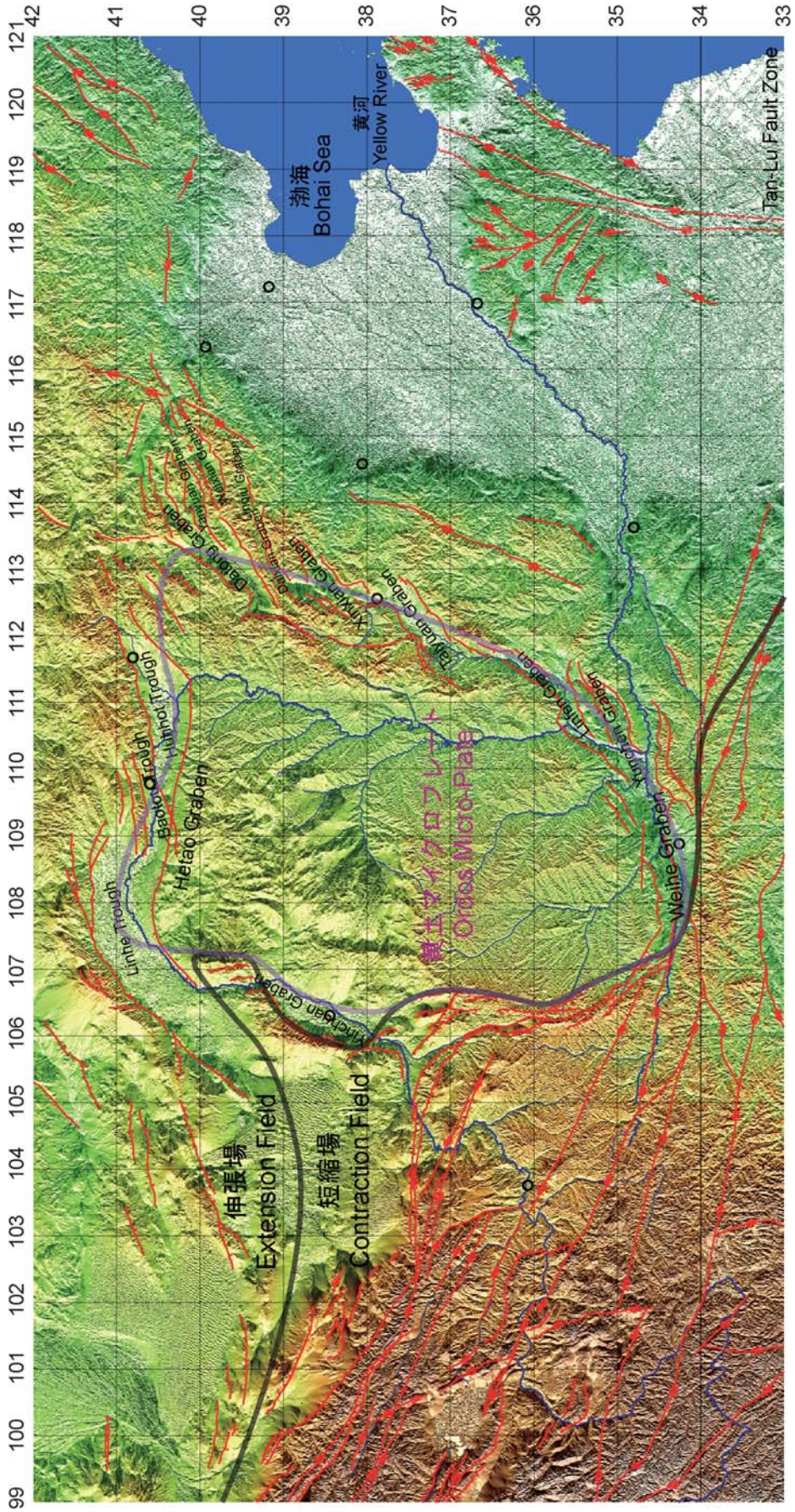

Fig. 11 Compiled major fault map of the Yellow River basin.

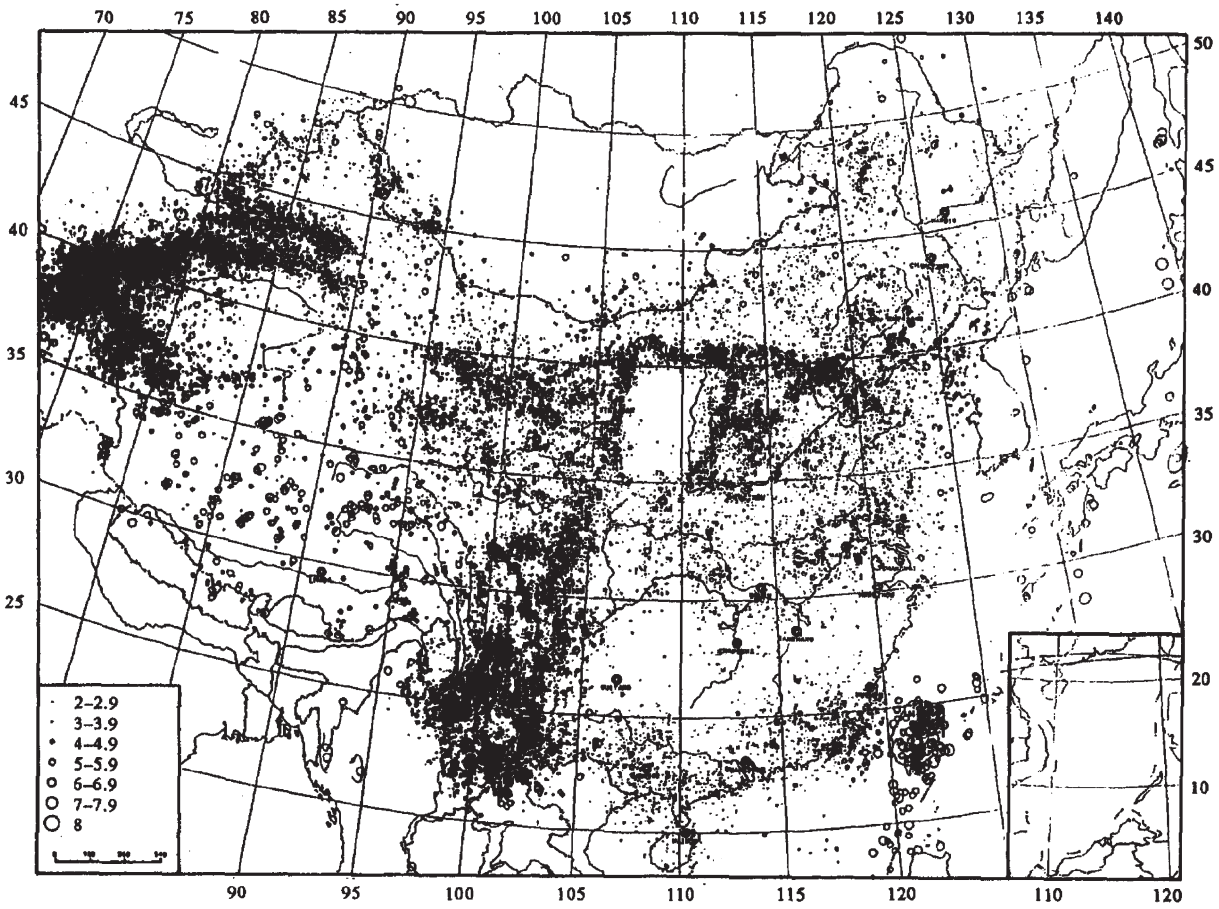

Fig. 12 Map of earthquake epicenters in Chin after Gao *et al*. (1995).

modeling and simulation for water resource management in the Yellow River basin, China. Bulletin of the Geological Survey of Japan, 60, 131-146.

Muraoka, H. and Ohtani, T. (2000) Profiling of the Kakkonda geothermal system by bulk rock chemistry of the well WD-1a. *Rept. Geol. Surv. Japan*, No. 284, 35-55 (in Japanese with English abstract).

Muraoka, H., Tateno, M. and Okubo, Y. (1999): Brittle-plastic transition penetrated by the well WD-1a beneath the Kakkonda geothermal field, Japan. *Geol. Surv. Japan Interim Report*, no.EQ/99/1, 66-68.

Muraoka, H., Uchida, T., Sasada, M., Yagi, M., Akaku, K., Sasaki, M., Yasukawa, K., Miyazaki, S.-I., Doi, N., Saito, S., Sato, K. and Tanaka, S. (1998): Deep geothermal resources survey program: igneous, metamorphic and hydrothermal processes in a well encountering 500 ºC at 3729 m depth, Kakkonda, Japan. *Geothermics*, **27**, 507-534.

Ritts, B.D., Darby, B.J. and Cope, T. (2001) Early Jurassic extensional basin formation in the Daqing Shan segment of the Yinshan belt, northern North China Block, Inner Mongolia. *Tectonophysics*, **339**, 239-358.

Shao, S. and Wang, M. (1989): Quaternary Map of Huang-Huai-Hai Plain in China 1:1,000,000 and Quaternary Lithofacies Paleogeographical Map of Huang-Huai-Hai Plain in China 1:2,000,000 with Explanatory Notes. Geological Publishing House, 66p.

Tapponnier, P., Xu, Z., Roger, F., Meyer, B., Arnaud, N., Wittinger, G. and Yang, J. (2001): Oblique stepwise rise and growth of the Tibet Plateau. *Science*, **294**, 1671-1677.

Wang, J and Ye, Z.R. (2006): Dynamic modeling for crustal deformation in China: Comparisons between the theoretical prediction and the recent GPS data. *Physics of the Earth and Planetary Interiors*, **155**, 201-207.

Zhang, Y.Q., Mercier, J.L. and Vergdly, P. (1998): Extension in the graben systems around the Ordos (China), and its contribution to the extrusion tectonics of south China with respect to Gobi-Mongolia. *Tectonophysics*, **285**, 41-75.

Zhang, Y.Q., Ma, Y., Yang, N., Shi, W. and Dong, S. (2003): Cenozoic extensional stress evolution in North China. *Journal of Geodynamics*, **36**, 591-613.

Received December, 15, 2008
Accepted December, 19, 2008

Bulletin of the Geological Survey of Japan, vol.60 (1/2), 2009

長期的地下水シミュレーションのための黄河流域の地質学的モデル

村岡洋文・森　康二・玉生志郎・石井武政・内田洋平

要　旨

黄河流域の全集水域における長期的地下水流動をシミュレートする目的で，水理地質学的モデルを構築した．このモデルは脆性ー塑性境界によって定義される不透水性基盤，上部地殻の浸透率の深度依存性の定式化，主要断層分布，および第四系の等層厚線図を含む．黄河流域は次の5つの階段状標高分布域に特徴づけられる．すなわち，チベット高原，チベット高原北東斜面，オルドス高原北西部，オルドス高原南東斜面，および華北盆地である．その構造はテクトニクス，とくに剛体的なオルドスマイクロプレートのテクトニクスに支配されている．適切な浸透率と局地的な地下水消費を仮定すれば，シミュレーションの結果は1960年代以降の地下水位の劇的な低下の記録とよく対応し，過剰な地下水消費がこの低下の主要な要因であることを示している．このモデルは黄河流域における地下水の将来の枯渇を予測することに使えるだろう．